IOP Publishing Journal of Physics: Condensed Matter

J. Phys.: Condens. Matter **23** (2011) 175304 (6pp) doi:10.1088/0953-8984/23/17/175304

Localization on a two-channel model with cross-correlated disorder

R C P Carvalho[1], M L Lyra[1], F A B F de Moura[1] and F Domínguez-Adame[2]

[1] Instituto de Física, Universidade Federal de Alagoas, Maceió-AL 57072-970, Brazil
[2] Departamento de Física de Materiales, Universidad Complutense, E-28040 Madrid, Spain

Received 3 February 2011, in final form 18 March 2011
Published 12 April 2011
Online at stacks.iop.org/JPhysCM/23/175304

Abstract

We study the wavepacket dynamics in a two-channel Anderson model with correlated diagonal disorder. To impose correlations in the disorder distribution we construct the on-site energy landscape following both symmetric and antisymmetric rules. Our numerical data show that symmetric cross-correlations have a small impact on the degree of localization of the one-particle eigenstates. In contrast, antisymmetric correlations lead to a reduction of the effective degree of disorder, thus resulting in a substantial increase of the wavepacket spread. A finite-size scaling analysis shows that the antisymmetric cross-correlations, in spite of weakening the localization, do not promote ballistic transport. The present results shed light on recent findings concerning an apparent delocalization transition in a correlated DNA-like ladder model.

1. Introduction

The wavepacket dynamics in a low-dimensional system is one of the main focuses of Anderson localization theory. The absence of extended eigenstates in low-dimensional systems with uncorrelated disorder has been predicted within the scope of perturbation theory and supported by scaling arguments [1]. Therefore the width of the time-dependent wavepacket localizes in a finite region around the initial position after a long-time run. More recently, it has been shown that low-dimensional disordered systems can support extended states or a localization–delocalization transition in the presence of short- or long-range correlations in the disorder distribution [2–17]. The effect of long-range correlated scatterers on the transport properties of microwave guides was experimentally studied and confirmed the presence of mobility edges [17]. Moreover, it was suggested that an appropriate algorithm for generating random correlated sequences with the desired mobility edges could be used in the manufacture of filters for electronic and optical signal processing [9].

The wavepacket dynamics in two-dimensional or multi-channel systems with correlated disorder is still an open issue with several connections to DNA geometry, semiconductors and superlattices. In particular, the simple problem of the electron dynamics in two-channel structures has been the focus of several works [18–22]. The well-known random dimer model [2] was generalized to the ladder case and a delocalized state at the band center was obtained [18]. Recently, an instructive debate about the possible existence of extended states in DNA-like two-channel models has emerged [20–22]. By using numerical calculations of the inverse participation ratio, it was claimed that a two-channel model based on DNA segments could support extended states [20]. Furthermore, on the basis of group theory arguments, it was proved that intrinsic-DNA correlations due to base pairing does not suffice to observe extended states [21]. Moreover, by using perturbation theory [22], a general formula was obtained for the localization length as a function of the autocorrelations along each channel and also the cross-correlations between the channels. In agreement with [21], it was proved that extended states cannot appear solely due to cross-correlations (e.g. DNA base paring). This discussion shows that the existence of extended states in the two-channel model or DNA-like model is still an open question.

More recently, it was shown that a quasiperiodic two-chain model can support extended states at multiple values of the Fermi energy [23]. Furthermore, it was demonstrated analytically that a two-channel random model can display a band of Bloch-type extended states when the on-site potentials and the hopping amplitudes display a particular correlation [24]. In [25] the effects of the coexistence of localized and extended states in the correlated random ladder model were investigated. By using numerical diagonalization and high-order methods to solve the Schrödinger equation, it was shown that stationary and dynamical properties are dominated by extended states. In addition, it was

 © 2011 IOP Publishing Ltd Printed in the UK & the USA

numerically demonstrated that the superposition of localized and delocalized bands gives rise to a new level-spacing distribution [25].

The aim of the present work is to elucidate the underlying physical mechanism behind the apparent delocalization transition exhibited by some models of correlated DNA-like tight-binding models [20]. Here, we will impose cross-correlations in the disorder distribution by introducing symmetric and antisymmetric rules between the on-site energies of each channel. The dynamics of an initially localized wavepacket will be investigated by numerically solving the time-dependent Schrödinger equation. Our numerical data show that, while symmetric cross-correlations have a small influence on the degree of localization, antisymmetric cross-correlations increase the wavepacket spread. A finite-size scaling analysis shows that antisymmetric cross-correlations, in spite of weakening the localization, do not promote ballistic transport. Theoretical explanations of the effect of cross-correlations in the wavepacket dynamics are provided.

2. Model and formalism

Our calculations make use of an effective tight-binding model Hamiltonian which describes the dynamics of an electron in a ladder geometry with correlated disorder. Considering a single orbital per site and nearest-neighbor interactions, the time-dependent Schrödinger equation (with $\hbar = 1$) is given by [21]

$$\mathrm{i}\,\frac{\mathrm{d}\psi_j^s}{\mathrm{d}t} = \epsilon_j^s\psi_j^s + V_\parallel(\psi_{j+1}^s + \psi_{j-1}^s) + V_\perp\psi_j^{\bar{s}}. \qquad (1)$$

Here $s = \pm 1$ labels each strand of the ladder and $\bar{s} = -s$ indicates its complementary. The index $j = 1, \ldots, N$ runs over the sites along one of the strands coupled by the hopping parameter $V_\parallel$. $V_\perp$ is the hopping parameter between complementary sites on each strand. The on-site cross-correlated energies ϵ_j^s will be generated as follows: ϵ_j^{+1} will be chosen as an uncorrelated random sequence with $\langle\epsilon_j^{+1}\rangle = 0$ and uniformly distributed within the interval $[-W, W]$ (we take $W = 1$ hereafter); the on-site energy of the other channel will be chosen as (a) $\epsilon_j^{-1} = \epsilon_j^{+1}$ or (b) $\epsilon_j^{-1} = -\epsilon_j^{+1}$. These distinct rules impose, respectively, symmetric and antisymmetric cross-correlations in the two-channel Hamiltonian.

We consider an electron initially localized at the orbital $|j_0 s_0\rangle$, namely, we take the initial condition $\psi_j^s(t = 0) = \delta_{jj_0}\delta_{ss_0}$. The set of equations above were solved numerically by using a high-order method based on the Taylor expansion of the evolution operator $V(\Delta t) = \exp(-\mathrm{i}H\Delta t) = 1 + \sum_{l=1}^{n_o}(-\mathrm{i}H\Delta t)^l/(l!)$, where H is the Hamiltonian. The wavefunction at time Δt is given by $|\Phi(\Delta t)\rangle = V(\Delta t)|\Phi(t = 0)\rangle$. The method can be used recursively to obtain the wavefunction at time t. To obtain $H^l|\Phi(t = 0)\rangle$, we will use a recursive formula. As a first step, we define $H^l|\Phi(t = 0)\rangle = \sum_{js}(C_j^s)^l|j, s\rangle$. Using the Schrödinger equation (1) we can compute $H^1|\Phi(t = 0)\rangle$ and obtain $(C_j^s)^1$ as

$$(C_j^s)^1 = \epsilon_j^s\psi_j^s + V_\parallel(\psi_{j+1}^s + \psi_{j-1}^s) + V_\perp\psi_j^{\bar{s}}. \qquad (2)$$

Therefore, using that $H^l|\Phi(t=0)\rangle = H\sum_{js}(C_j^s)^{l-1}|j, s\rangle$, $(C_j^s)^l$ can be obtained recursively as

$$(C_j^s)^l = \epsilon_j^s(C_j^s)^{l-1} + V_\parallel[(C_{j+1}^s)^{l-1} + (C_{j-1}^s)^{l-1}] + V_\perp(C_j^{\bar{s}})^{l-1}. \qquad (3)$$

Results were obtained by using $\Delta t = 0.5$ and the sum was truncated at $n_o = 20$. This cutoff was sufficient to keep the wavefunction norm conservation along the entire time interval considered. This formalism is faster than high-order Runge–Kutta methods and it is easier to implement. We are particularly interested in the square root of the mean-square displacement $\sigma(t)$ defined by

$$\sigma(t) = \sqrt{\sum_{j,s}[(j - j_0)^2 + (s - s_0)^2]|\psi_j^s(t)|^2}. \qquad (4)$$

$\sigma(t)$ gives an estimate of the width of the wavepacket at time t. In the long-time regime its scaling behavior can also be used to distinguish between localized and delocalized wavepackets [21]. In addition we compute the Lyapunov exponent $\gamma(E)$ (which is the inverse of the localization length Λ) of long two-channel segments by means of the following equation:

$$\gamma(E) = 1/\Lambda(E) = (1/2N)\ln\left[\mathrm{Tr}\left|G_{1,N+1}^{N+1}\right|^2\right], \qquad (5)$$

where $G_{1,N+1}^{N+1}$ denotes the Green's function operator between the first and the $(N + 1)$th pair of sites. To compute this operator, we use a standard recursion method (see [26] for details). For extended states, $1/\Lambda(E)$ vanishes in the thermodynamic limit.

3. Results

The numerical solution of the time-dependent Schrödinger equation was performed on two-channel systems with $N = 1000$ up to 16 000 sites on each strand. Numerical convergence was ensured by conservation of the norm of the wavepacket at every time step, i.e. $|1 - \sum_{js}|\psi_j^s(t)|^2| < 10^{-10}$. All calculations were averaged over 30 disorder configurations, which were enough to keep statistical fluctuations much smaller than the average value of all physical quantities investigated. In figure 1 we plot the time-dependent wavepacket width σ versus time t computed using $N = 4000$ sites, $V_\parallel = V_\perp = 1$, both kinds of cross-correlations and a standard uncorrelated random two-channel system. We can see that antisymmetric cross-correlations, $\epsilon_j^{-1} = -\epsilon_j^{+1}$ (see the dotted line), produce a localization degree much weaker than the other cases (see the solid line data for $\epsilon_j^{-1} = \epsilon_j^{+1}$ and the dashed line for the uncorrelated case). In figure 2 we offer a comparative numerical analysis between both types of cross-correlations by considering the scaled wavepacket width σ/N versus scaled time t/N. Calculations were done using $V_\parallel = V_\perp = 1$ and $N = 1000$ up to 16 000 sites. For extended states, data from distinct chain sizes would collapse into a single curve, signaling a ballistic transport ($\sigma \propto t$). In our case, both calculations show no data collapse. Furthermore, the scaled asymptotic wavepacket width decreases as the system

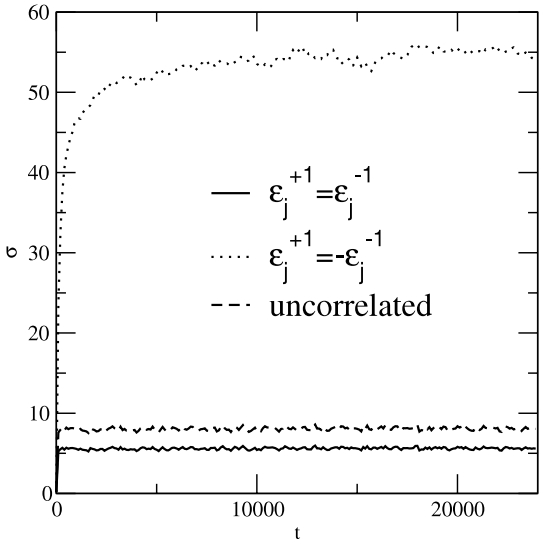

Figure 1. The time-dependent wavepacket width σ versus time t. Calculations were done using $N = 4000$ and considering distinct kinds of cross-correlations within diagonal disorder. Antisymmetric cross-correlations $\epsilon_j^{-1} = -\epsilon_j^{+1}$ lead to a wavepacket width much larger than that one produced by symmetric cross-correlations $\epsilon_j^{-1} = \epsilon_j^{+1}$.

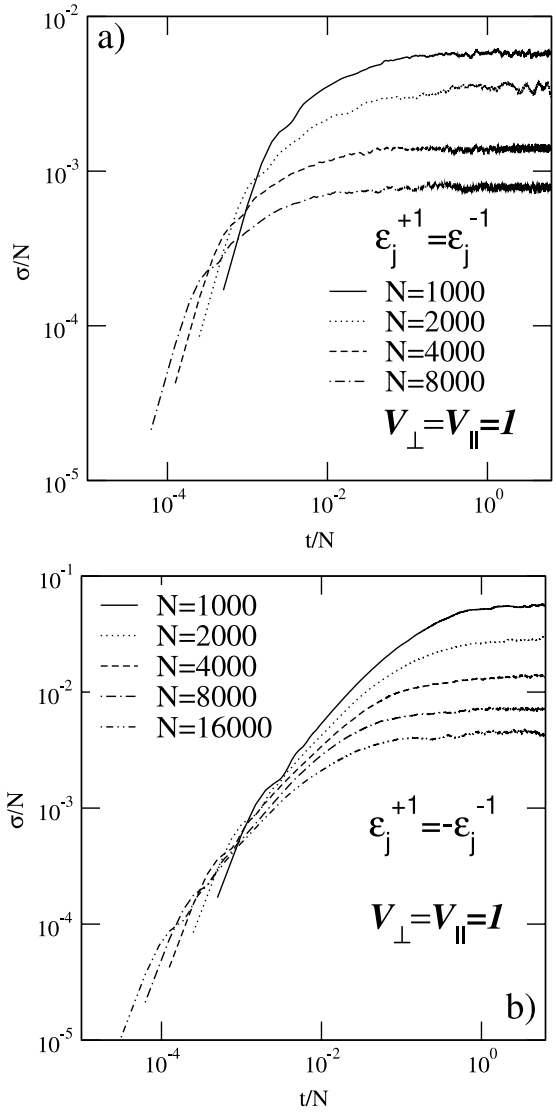

Figure 2. Scaled wavepacket width σ/N versus scaled time t/N. Calculations were done using $V_\parallel = V_\perp = 1$ and $N = 1000$ up to 16 000 sites. Our calculations indicate that the asymptotic scaled wavepacket width $\sigma/N \to 0$ as N increases for both cross-correlations used here, a typical signature of localized wavepackets.

size increases, pointing to an ultimate localization of the wavepacket in the thermodynamic limit. Therefore, the cross-correlations used here do not induce the emergence of truly extended states. These results agree with previous calculations found in [21, 22], confirming that diagonal cross-correlations are not sufficient to promote a metal–insulator transition in a two-channel disordered Hamiltonian.

However, it is clear in both figures 1 and 2 that antisymmetric cross-correlation $\epsilon_j^{-1} = -\epsilon_j^{+1}$ leads to a wavepacket spread much larger than the symmetric case ($\epsilon_j^{-1} = \epsilon_j^{+1}$). Let us stress that antisymmetric cross-correlation contains the same ingredients used in the generic DNA model studied in [20], i.e. when $\langle \epsilon_j^{-1} + \epsilon_j^{+1} \rangle = 0$. We will show additional data and theoretical arguments to unveil the origin of the substantial decrease of the degree of localization and the apparent phase transition found in [20] in the two-channel model with antisymmetric diagonal cross-correlations.

Let us first analyze in closer detail the two-channel model with symmetric cross-correlated disorder. The Hamiltonian model of an isolated dimer pair has eigenenergies given by $\epsilon_j \pm V_\perp$. In the regime of strong inter-chain coupling these two modes cannot be efficiently mixed by the intra-chain coupling. Therefore the system shall behave as two uncoupled random chains with energy offset given by $\pm V_\perp$ and the disorder strength is simply the one originally present in the on-site energies. Within this scenario, the degree of localization shall be similar to the one present in the system without cross-correlations. On the other hand, the Hamiltonian model of an isolated dimer pair with antisymmetric diagonal terms has eigenenergies given by $\pm\sqrt{\epsilon_j^2 + V_\perp^2}$. In the regime of strong inter-chain coupling these can be written as $\pm V_\perp + \epsilon_j^2/2V_\perp$. Also in this case, these modes are not effectively mixed by the intra-chain coupling and the system shall behave as two independent random chains. However, the effective disorder is rescaled. It becomes of the order of $1/V_\perp$. Recalling that the localization length in random chains is proportional to the square of the inverse disorder width, antisymmetric cross-correlations shall have exponentially localized states whose localization length grows with $V_\perp^2$ in the regime of strongly coupled chains.

In order to corroborate the above picture, we will provide additional numerical data of the wavepacket width, density of states and localization length of the energy eigenmodes for both models with cross-correlated disorder, as well as for the two-channel model with uncorrelated disorder. In figure 3(a) we plot the wavepacket width $\sigma(t)$ versus time t for $N = 4000$, antisymmetric cross-correlations $\epsilon_j^{-1} = -\epsilon_j^{+1}$, $V_\parallel = 1$ and $V_\perp = 1$ up to 5. The results show that the wavepacket spread

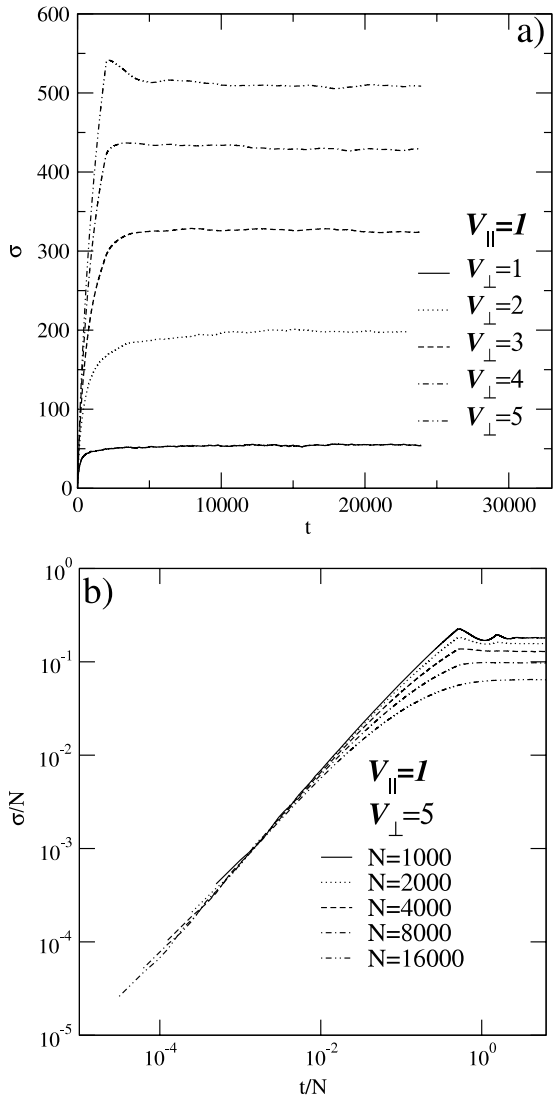

Figure 3. (a) The wavepacket width $\sigma(t)$ versus time t for $N = 4000$, $\epsilon_j^{-1} = -\epsilon_j^{+1}$, $V_\parallel = 1$ and $V_\perp = 1$ up to 5. When the intra-chain hopping $V_\perp$ is increased in two-channel systems with antisymmetric cross-correlations $\epsilon_j^{-1} + \epsilon_j^{+1} = 0$, the local effective disorder along the quasi-unidimensional system goes to zero, thus increasing the localization length. (b) Scaled spread σ/N versus scaled time t/N for $V_\parallel = 1$, $N = 1000$ up to 16 000 sites and $V_\perp = 1$ up to 5 and $N = 1000$ up to 16 000 sites. In spite of the fact that antisymmetric cross-correlations favor the increase of the localization length, it does not lead to truly extended wavepackets once $\sigma/N \to 0$ as N increases.

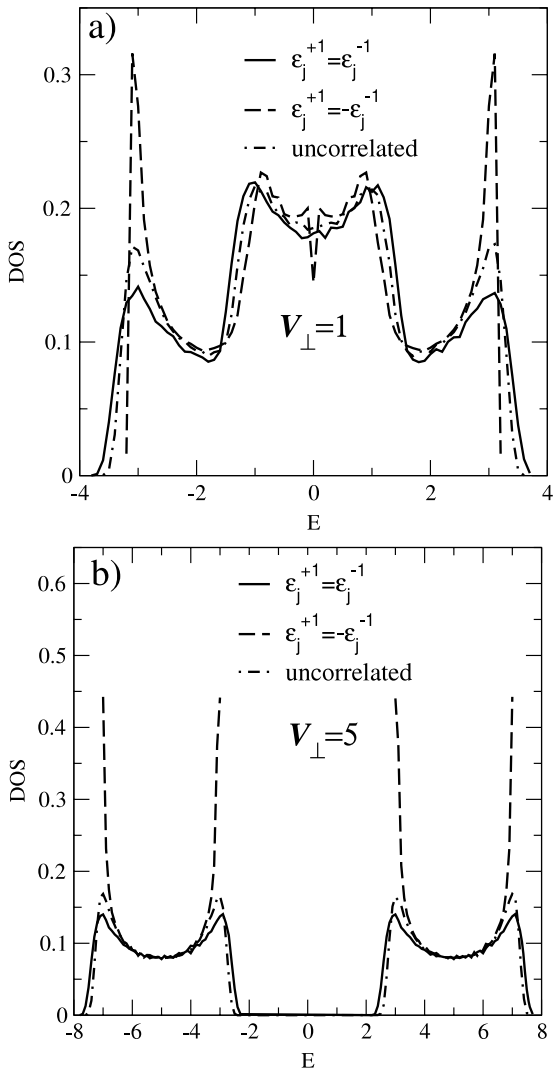

Figure 4. (a) The normalized density of states DOS(E) versus energy E computed using $N = 5000$ sites, 500 disorder configurations and (a) $V_\perp = 1$ and (b) $V_\perp = 5$. When the intra-chain hopping $V_\perp$ is increased in two-channel systems with antisymmetric cross-correlations $\langle \epsilon_j^{-1} + \epsilon_j^{+1} \rangle = 0$, the density of states becomes similar to the DOS of two uncoupled perfect chains with on-site energies $V_\perp$ and $-V_\perp$. Symmetric cross-correlations produce a DOS with rounded band edges, signaling that the underlying disorder remains relevant even in the regime of strong intra-chain coupling.

increases as the intra-chain coupling $V_\perp$ is also increased. However, even in the regime of strong intra-chain coupling $V_\perp$, the asymptotic scaled spread σ/N decreases with the system size, indicating an ultimate localization in the thermodynamic limit. Let us stress again that the calculations in [20] were done by using a two-channel system with a strong intra-chain coupling $V_\perp > V_\parallel$. Therefore, the reduction on the degree of localization reported in [20] actually reflects the weakening of the effective disorder in the two-channel system with antisymmetric cross-correlations and strong intra-chain hopping. However, this specific cross-correlation does not promote the emergence of truly extended states.

To further illustrate the above point, we provide some results from the exact diagonalization of the present two-channel Hamiltonian models. We show in figure 4 the normalized density of states (DOS(E) $= \sum_{E_n} \delta(E - E_n)$, where E_n are the eigenvalues obtained from numerical diagonalization) versus energy E. Calculations were done using $N = 5000$ sites, 500 disorder configurations, and $V_\perp = 1$ and $V_\perp = 5$ (see figures 4(a) and (b)). When the intra-chain and inter-chain couplings are of the same order, the DOS displays a single band which starts to split in a two-band structure when the intra-chain coupling is increased. We already notice that, even in this regime of intermediate intra-chain coupling, the band edges in the presence of antisymmetric cross-correlations are sharper than in the other

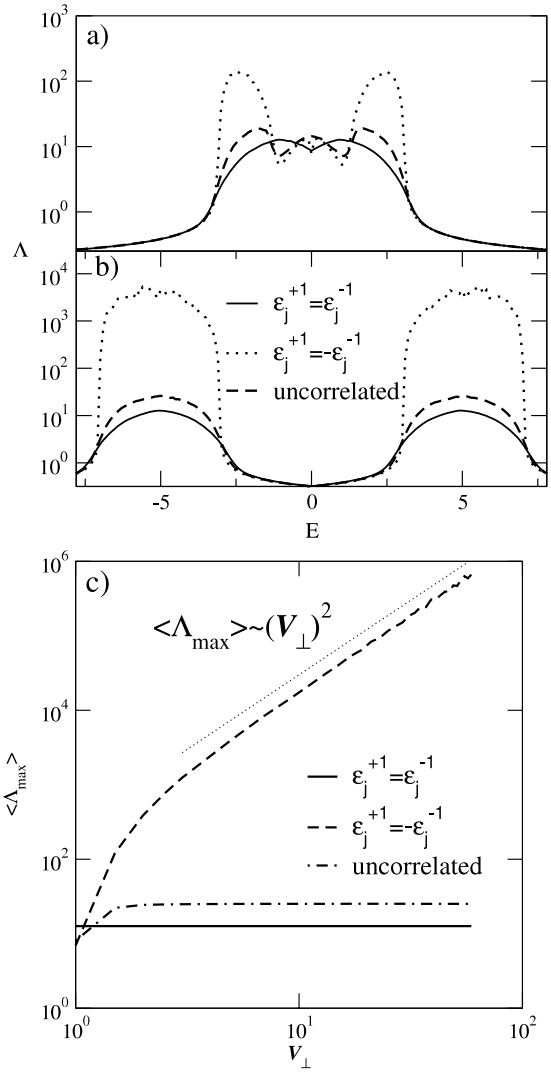

Figure 5. ((a), (b)) The localization length Λ versus energy E computed using $N = 10^7$ sites, both kinds of cross-correlations and a standard uncorrelated random two-channel system. Calculations were done using $V_\parallel = 1$: (a) $V_\perp = 1$ and (b) $V_\perp = 5$. (c) The largest localization length Λ_{max} versus intra-chain hopping $V_\perp$. The localization length diverges with $(V_\perp)^2$ in two-channel systems with antisymmetric cross-correlations while it remains finite in the other two cases.

cases. For large intra-chain hopping, the density of states of the two-channel systems with symmetric cross-correlations is quite similar to the one displayed by the corresponding uncorrelated model. The DOS in these two cases resembles the one of two uncoupled chains with a finite disorder width, signaled by the rounding of the band edges. On the other hand, the DOS of the model with antisymmetric cross-correlations displays quite sharp band edges in the limit of strong intra-chain coupling which is consistent with the vanishing of the effective disorder.

In figure 5 we plot the localization length Λ versus energy E computed using $N = 10^7$ sites for both kinds of cross-correlations and a standard uncorrelated random two-channel system. We consider $V_\parallel = 1$ and $V_\perp = 1$ and 5. Notice that, even in the regime of intermediate intra-chain coupling, the localization length near the band edges is one order of magnitude larger in the presence of antisymmetric cross-correlations when compared with the other two cases. This effect becomes much more pronounced in strongly coupled channels. In figure 5(c) we plot the larger localization length Λ_{max} versus the intra-chain hopping $V_\perp$. The localization length diverges as $(V_\perp)^2$ in two-channel systems with antisymmetric cross-correlations, while symmetric cross-correlations have a small influence on the degree of localization. These numerical results corroborate our theoretical arguments given above.

4. Summary and conclusions

In this work we revisited the problem of electronic wavepacket dynamics in two-channel disordered structures. We considered an Anderson Hamiltonian in a quasi-unidimensional geometry (a two-channel geometry). In particular, we studied in detail two distinct types of two-channel models with cross-correlations within the diagonal disorder. By following the time evolution of an initially localized wavepacket, we showed that quasi-unidimensional structures with diagonal disorder displaying local correlations do not support truly extended states. In addition, we showed that symmetric cross-correlations ($\epsilon_j^{-1} = \epsilon_j^{+1}$) have a very limited influence on the degree of localization. In contrast, antisymmetric cross-correlations ($\epsilon_j^{-1} = -\epsilon_j^{+1}$) substantially inhibit the Anderson localization, especially in the regime of strongly coupled chains. It is interesting to stress that the role of symmetric and antisymmetric correlations has been previously investigated in the context of Coulomb-correlated electron–hole pairs in disordered semiconductors [27, 28]. It has been shown that the delocalization action of the Coulomb potential is also stronger for antisymmetrically correlated electron–hole site energies, in close correspondence with our present results. The physical mechanism underlying the phenomenology reported here was revealed by stressing that, in the regime of strong inter-chain couplings, the energy eigenmodes can be roughly decoupled in those of two independent random chains with symmetric energy offsets. While symmetric cross-correlations keep the strength of the effective disorder finite, antisymmetric cross-correlations leads to a rescaled disorder width which vanishes as the inter-chain coupling increases. Such reduction of the effective disorder is reflected in the localization length of the energy eigenmodes, which can surpass 10^3 base pairs even for moderate inter-chain couplings. Therefore, these states behave as effectively extended in small systems, leading to an apparent metal–insulator phase transition [20].

Acknowledgments

This work was partially financed by the Brazilian research agencies CAPES (PROCAD, Rede NanoBioestruturas), CNPq (INCT-Nano(Bio)Simes, project no. 573925/2008-9) and FAPERN/CNPq (Pronex). Work at Madrid was supported by MEC (projects MOSAICO and MAT2010-17180). FABFdM would like to thank the hospitality of Departamento de Física de Materiales (UCM).

References

[1] Abrahams E, Anderson P W, Licciardello D C and Ramakrishnan T V 1979 *Phys. Rev. Lett.* **42** 673

[2] Dunlap D H, Wu H L and Phillips P W 1990 *Phys. Rev. Lett.* **65** 88
Wu H-L and Phillips P 1991 *Phys. Rev. Lett.* **66** 1366

[3] Domínguez-Adame F, Maciá E and Sánchez A 1993 *Phys. Rev.* B **48** 6054

[4] Varga I and Pipek J 1998 *J. Phys.: Condens. Matter* **10** 305

[5] de Moura F A B F and Lyra M L 1998 *Phys. Rev. Lett.* **81** 3735

[6] de Moura F A B F, Coutinho-Filho M D, Raposo E P and Lyra M L 2002 *Phys. Rev.* B **66** 014418

[7] de Moura F A B F, Coutinho-Filho M D, Raposo E P and Lyra M L 2003 *Phys. Rev.* B **68** 012202

[8] Domínguez-Adame F, Malyshev V A, de Moura F A B F and Lyra M L 2003 *Phys. Rev. Lett.* **91** 197402

[9] Izrailev F M and Krokhin A A 1999 *Phys. Rev. Lett.* **82** 4062
Izrailev F M, Krokhin A A and Ulloa S E 2001 *Phys. Rev.* B **63** 41102

[10] Zhang G P and Xiong S-J 2002 *Eur. Phys. J.* B **29** 491

[11] de Moura F A B F, Coutinho-Filho M D, Raposo E P and Lyra M L 2004 *Europhys. Lett.* **66** 585

[12] Bellani V, Diez E, Hey R, Toni L, Tarricone L, Parravicini G B, Domínguez-Adame F and Gómez-Alcalá R 1999 *Phys. Rev. Lett.* **82** 2159

[13] Shima H, Nomura T and Nakayama T 2004 *Phys. Rev.* B **70** 075116

[14] Schubert G, Weiße A and Fehske H 2005 *Physica* B **359–361** 801

[15] Liu W S, Chen T and Xiong S J 1999 *J. Phys.: Condens. Matter* **11** 6883

[16] de Moura F A B F, Lyra M L, Domínguez-Adame F and Malyshev V A 2007 *J. Phys.: Condens. Matter* **19** 056204

[17] Kuhl U, Izrailev F M, Krokhin A and Stöckmann H J 2000 *Appl. Phys. Lett.* **77** 633

[18] Sedrakyan T and Ossipov A 2004 *Phys. Rev.* B **70** 214206

[19] Tessieri L and Izrailev F M 2006 *J. Phys. A: Math. Gen.* **39** 11717

[20] Caetano A and Schulz P A 2005 *Phys. Rev. Lett.* **95** 126601

[21] Sedrakyan A and Domínguez-Adame F 2006 *Phys. Rev. Lett.* **96** 059703
Díaz E, Sedrakyan A, Sedrakyan D and Domínguez-Adame F 2007 *Phys. Rev.* B **75** 014201

[22] Bagci V M K and Krokhin A A 2007 *Phys. Rev.* B **76** 134202

[23] Sil S, Maiti S K and Chakrabarti A 2008 *Phys. Rev. Lett.* **101** 076803

[24] Sil S, Maiti S K and Chakrabarti A 2008 *Phys. Rev.* B **78** 113103

[25] de Moura F A B F, Caetano R A and Lyra M L 2010 *Phys. Rev.* B **81** 125104

[26] Kramer B and MacKinnon A 1993 *Rep. Prog. Phys.* **56** 1469

[27] Thomas P, Varga I, Lemm T, Golub J E, Maschke K, Meier T and Koch S W 2000 *Phys. Status Solidi* b **218** 125

[28] Schlichenmaier C, Varga I, Meier T, Thomas P and Koch S W 2002 *Phys. Rev.* B **65** 085306